ERS AND ENVISAT DIFFERENTIAL SAR INTERFEROMETRY FOR SUBSIDENCE MONITORING

Urs Wegmüller[1], Tazio Strozzi[1], and Luigi Tosi[2]

[1]Gamma Remote Sensing, Thunstrasse 130, CH-3074 Muri b. Bern, Switzerland
Tel: +41 31 951 70 05, Fax: +41 31 951 70 08, Email: wegmuller@gamma-rs.ch

[2]Istituto per lo Studio della Dinamica delle Grandi Masse, CNR
30125 Venezia, Italy

ABSTRACT

This paper reports on the potential of differential SAR interferometry to map land subsidence. After a presentation of the methodology, the focus will be on feasibility demonstration and accuracy assessment. The theoretical considerations are verified with the selected cases Ruhrgebiet, Mexico City, Bologna, and Euganean Geothermal Basin, representing fast (*m/year*) to slow (*mm/year*) deformation velocities.

The accuracy of the generated deformation maps and the maturity of the required processing techniques lead to the conclusion that differential SAR interferometry has a very high potential for operational mapping of land subsidence. The high reliability of the ERS satellites, with the huge data archive starting in 1991, strongly supports this application. The planned ENVISAT ASAR has the potential to maintain good data availability into the future. This will, nevertheless, strongly depend on the sensor operation strategy.

Keywords: subsidence, SAR interferometry, ERS, ENVISAT

INTRODUCTION

The potential of differential Synthetic Aperture Radar (SAR) interferometry to map coherent displacement at c*m* to *mm* resolution resulted in spectacular new results for geophysical sciences. Earthquake displacement [1], volcano deformation [2], glacier dynamics [3], and land subsidence [4-7] were mapped. The required data are provided by the space-borne SAR sensors on the ERS-1, ERS-2, Radarsat, and JERS satellites. The planned follow-on sensors on ENVISAT and ALOS have the potential to ensure the availability of appropriate data into the future.

The objectives of this contribution are the presentation of the SAR interferometric methodology and the assessment of its performance for fast to slow subsidence velocities.

DIFFERENTIAL SAR INTERFEROMETRY

The phase difference ϕ of two SAR images acquired from almost the identical aspect angles is related to the imaging path length difference

$$\phi = -\frac{4\pi}{\lambda}\left(|\mathbf{r_2}| - |\mathbf{r_1}|\right), \tag{1}$$

where λ is the radar signal wavelength. The phase is determined as the argument of the normalized interferogram, γ, defined as the normalized complex correlation coefficient of the complex backscatter intensities s_1 and s_2 at positions $\mathbf{r_1}$ and $\mathbf{r_2}$

$$\gamma = \frac{\langle s_2 s_1{}^* \rangle}{\sqrt{\langle s_1 s_1{}^* \rangle \langle s_2 s_2{}^* \rangle}}, \tag{2}$$

with the brackets $\langle x \rangle$ standing for the ensemble average of x. The variance of the estimate of the interferometric phase ϕ is reduced by coherent averaging over statistically independent samples. The degree of coherence, a measure of the phase noise, is defined as the magnitude of the normalized interferogram $\gamma = |\gamma|$.

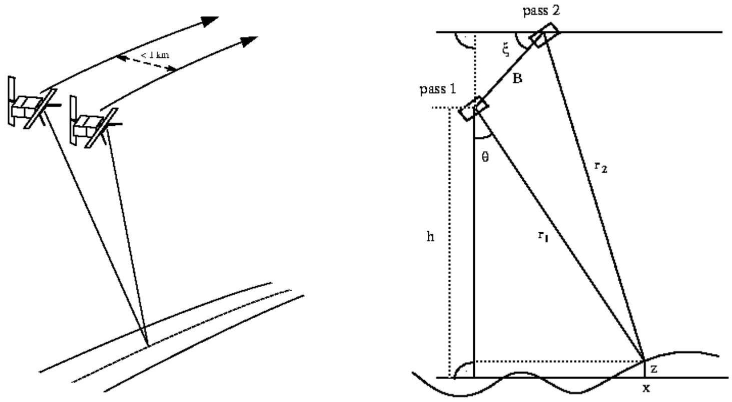

Figure 1: Interferometric imaging geometry showing the two passes with range vectors $\boldsymbol{r_1}$ and $\boldsymbol{r_2}$ to the resolution element. The look angle of the radar is θ. The baseline B is tilted at an angle ξ measured relative to horizontal.

The interferometric imaging geometry formed by two passes of a radar sensor separated by the baseline *B* is shown in Figure 1. The interferometric phase is sensitive to both surface topography and coherent displacement along the look vector occurring between the acquisition of the interferometric image pair. Inhomogeneous propagation delay and phase noise are the main error sources. The unwrapped interferometric phase ϕ_{unw} can be expressed as a sum of a topographic term φ_{topo}, a displacement term φ_{disp}, a path delay term φ_{path}, and a phase noise (or decorrelation) term ϕ_{noise}:

$$\phi_{unw} = \phi_{topo} + \phi_{disp} + \phi_{path} + \phi_{noise} \,. \tag{3}$$

The phase to height sensitivity,

$$\delta\phi_{topo} = \frac{4\pi}{\lambda} \frac{B_{\perp}}{r \cdot sin\theta} \delta h \,, \tag{4}$$

with the wavelength, λ, the baseline component perpendicular to the look vector, $B_{\perp}$, the incidence angle, θ, and the slant range, r, characterizes the topographic term. Knowing the baseline geometry and ϕ_{topo} allows to calculated the exact look angle and together with the orbit information the position of the scatter elements allowing to derive the surface topography.

The displacement term, ϕ_{disp}, is related to the *coherent* displacement of the scattering centers along the radar look vector, r_{disp}:

$$\phi_{disp} = 2kr_{disp} \,, \tag{5}$$

where *k* is the wavenumber. In this context *coherent* means that the same displacement is observed for adjacent scatter elements. Under the assumption of exclusively vertical displacement Equation 5 can be converted to

$$\phi_{disp} = \frac{2kr_{sub}}{cos\theta} \,, \tag{6}$$

where r_{sub} is the vertical displacement. The sensitivity of ϕ_{disp} to surface deformation is very high. In the case of ERS, for example, 2π displacement phase corresponds to only 2.7 *cm* displacement along the look vector or 3 *cm* of vertical subsidence. Vertical subsidence can usually be assumed in the case of ground water extraction. In the case of mining induced subsidence, on the other hand, the observed geometry of the ground movement is more complicated. Even a combination of SAR data acquired in ascending and descending mode does not allow to resolve the complete three dimensional displacement vector field, without use of additional information.

The path delay term ϕ_{path} is the result of spatial inhomogeneity in the atmospheric conditions (mainly water vapor content). An approach to improve the ratio between the subsidence signal and the atmospheric phase error is the stacking of multiple interferograms [8,9]. Under the assumption of a stationary process the subsidence term adds up linearly, i.e. the addition of the unwrapped phases of two interferograms with one and two years acquisition intervals results in an unwrapped phase covering an effective time interval of 3 years. For the error term, on the other hand, statistical independence between independent interferograms can be assumed resulting in an increase with the square root of the number of pairs. The relative subsidence velocity estimation error is calculated as

$$\frac{\Delta r_{sub}}{r_{sub}} = \frac{\sqrt{n} \cdot E}{v \cdot \sum t_i}. \tag{7}$$

with n the number of independent interferograms used, E the absolute error estimate for a single interferogram, v the subsidence velocity, and $\sum t_i$ the cumulative time interval. Equation 7 can also be used to determine the cumulative time required to map a certain subsidence velocity with a predefined expected relative estimation error. The potential of the interferogram stacking technique is demonstrated by the fact that the stacking of more than 10 independent interferograms allowing to reach a cumulative time interval of more than 20 years results in an expected subsidence velocity estimation error below 1 *mm/year*. Such stacking is indeed possible thanks to the immense ERS data archive.

The decorrelation term ϕ_{noise} is caused by random (or incoherent) displacement of the scattering centers and by SAR signal noise. Multi-looking and filtering of the interferogram allow to reduce the phase noise. The main difficulty with high phase noise is not so much the statistical error introduced in the estimation of ϕ_{topo} and φ_{disp} but resulting phase unwrapping problems. Ideally, the phase noise and the phase difference between adjacent pixels are both much smaller than π. In reality this is often not the case, especially for areas with a low coherence and rugged topography. The coherence of ERS Tandem pairs (1 day acquisition time interval) is very low for open water and forest and higher for most other classes. For a 35 day time interval the coherence is still quite high over sparsely vegetated terrain. For acquisition intervals longer than one year the areas with higher coherence levels are further reduced mainly to urban and sub-urban areas.

The basic idea of the differential interferometric approach is to separate the effects of surface topography and coherent displacement, allowing to retrieve differential displacement maps [10] This goal is achieved by subtracting the topography related phase, ϕ_{topo}, which is either calculated based on a available Digital Elevation Model (DEM) or estimated from an independent interferogram with a short acquisition interval, such as an ERS Tandem pair. In many cases the use of a DEM turns out to be more robust and operational. The phase unwrapping required in the multi-pass approach is often difficult to resolve and far from operational for low coherence areas, especially in rugged terrain. In addition, gaps in the unwrapped topographic phase for areas of too low coherence may be present, depending on the phase unwrapping method used. Because of the scaling of the topographic phase with the perpendicular baseline component (Equation 4) the accuracy of baseline estimation is very important. At present we use various estimation methods based on the orbits data, the registration offsets, and the fringe rate of the interferogram. The error in a displacement measurement resulting from inaccurate baseline increases with the size of the area investigated.

Data processing related aspects which influence the robustness and operationality of the application as well as the accuracy of the result include phase filtering, phase unwrapping, geocoding, and the averaging scheme for multiple results. More details on the processing chain used for the generation of the results presented in this paper are found in [11].

Table 1: Subsidence velocities for the selected sites. In all cases SAR data of the European Remote Sensing Satellites ERS-1 and ERS-2 were used.

	Velocities *[cm/year]*	Monitoring interval	Interferograms / Cumulative time	Expected accuracy[1] *[cm/year]*
Ruhrgebiet (Germany)	0 - 200	1 month	1 / 1 month	9.0
Mexico City (Mexico)	0 - 40	3 months	1 / 3 months	3.0
Bologna (Italy)	0 - 4	1 year	6 / 4 years	0.5
Euganean Geothermal Basin (Italy)	0 - 0.4	5 years	10 / 20 years	0.1

[1] as calculated for an assumed atmospheric distortion of $\pi/2$. No other errors considered.

EXAMPLES

Four sites characterized by different displacement velocities were selected to investigate the performance of differential SAR interferometry for land subsidence monitoring: the Ruhrgebiet (Germany), Mexico City (Mexico), Bologna (Italy), and the Euganean Geothermal Basin (Italy). The approximate subsidence velocities, the monitoring interval selected, the number of interferograms used and the expected estimation error are summarized in Table 1. In the following the results achieved for the four sites will be summarized.

Ruhrgebiet

Coal mining causes significant surface movement in the German Ruhrgebiet. Due to legal requirements the mining companies are obliged to assess the environmental impact of the excavations. Surface deformation caused by mining is a very dynamic process with high spatial and temporal variability. For mining areas with high subsidence velocities, interferometric pairs with acquisition intervals of only one or a few 35 day repeat cycles are preferred. Subsidence maps of different time intervals clearly indicate the progress in the sub-surface coal excavation. Figure 2 shows an example of a typical deformation cone observed for areas of active excavation. The colors indicate the deformation along the SAR observation direction. One color cycle corresponds to a displacement of 2.7 *cm* during the 35 days time interval. Vertical subsidence cannot be assumed in this case of mining induced deformation. The white color indicates areas of low coherence where the phase could not be unwrapped. Validation with excavation plans, levelling data and theoretical models confirmed the good accuracy and usefulness of SAR interferometry for the monitoring of mining induced surface deformation [7].

Mexico City

Mexico City is built on highly compressible clays and by reason of strong groundwater extraction a total subsidence of more than nine meters has been observed over the last century. The selection of ERS data to map subsidence at Mexico City is strongly restricted by the relatively few acquisitions found in the archive. From the available data acquisitions, three independent differential interferograms, one in ascending and two in descending mode, were selected. The subsidence maps derived from the three independent interferograms were found to be consistent [4]. For the period January 1996 – May 1996 (Figure 3) the observed maximum subsidence velocities are about 40cm/year, in general agreement with those reported in the literature and derived form levelling surveys and theoretical models.

Bologna

At Bologna, Italy, the subsiding area is large with maximum subsidence velocities of 6 to 8 *cm/year* and characteristic spatial gradients of the vertical movement. Levelling surveys are being conducted at intervals of several years. We decided to use this case to investigate the potential of differential SAR interferometry because of the large science community involved in this case and the available reference data which can be used for validation purposes.

Two subsidence maps for the time periods 1992-1993 (Figure 4a) and 1997-1998 (Figure 4b) using in both cases six ERS SAR data and the interferogram stacking technique were produced. The results of differential SAR interferometry are in very good agreement with those derived from levelling surveys. For 215 points distributed over the urban area of Bologna the average difference between the SAR interferometric subsidence results of the time period 1992-1993 and the levelling data of 1987 and 1991 is 0.4 cm/year with a standard deviation of 0.9 cm/year. The minimum and maximum differences are –3.7 and +2.6 cm/year, respectively. The small standard deviation of 0.9 cm/year between the data of the two methods indicates a good performance of ERS differential SAR interferometry for subsidence mapping in urban areas. The systematic offset between the two data sets can be explained by the different time period, indicating a decrease of the subsidence velocity. More recent levelling data acquired in the summer of 1999 will be used for a more direct validation, as soon as these data will become available. A more detailed description of this case is given by [6].

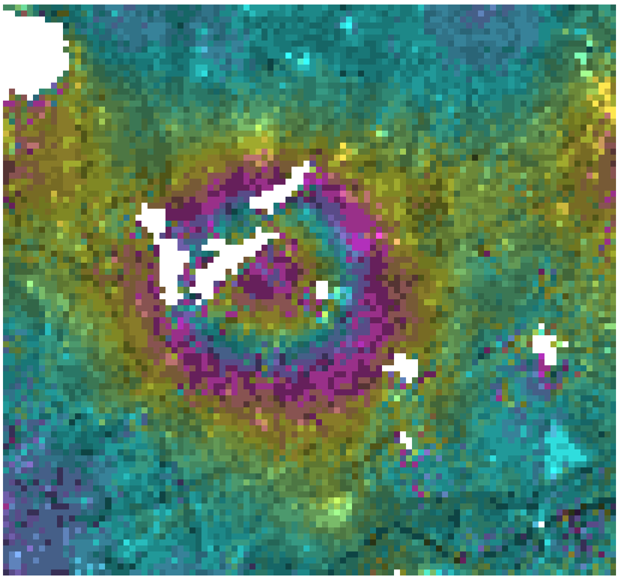

Figure 2. Ruhrgebiet: deformation map for active coal excavation site. The image width is 2.5 *km*. The color scale is defined in the text. For the image brightness the backscattering coefficient is used.

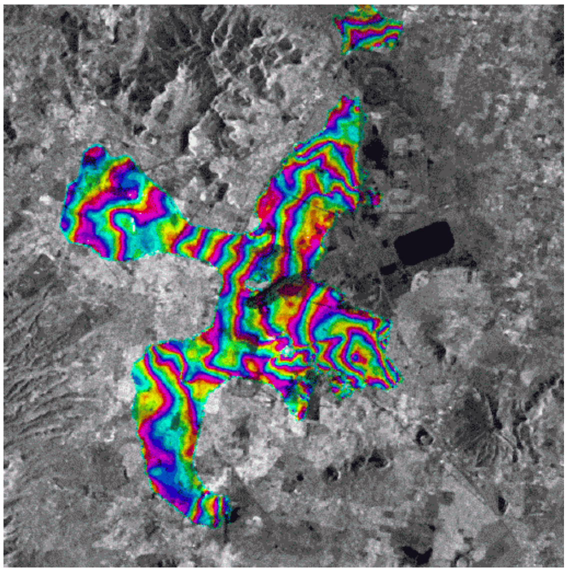

Figure 3. Mexico City: interferometric subsidence map derived from the ERS pair 29-Dec-1995 / 16-May-1996. Subsidence velocity per color cycle: 5 *cm/year*. For the image brightness the backscattering coefficient is used.

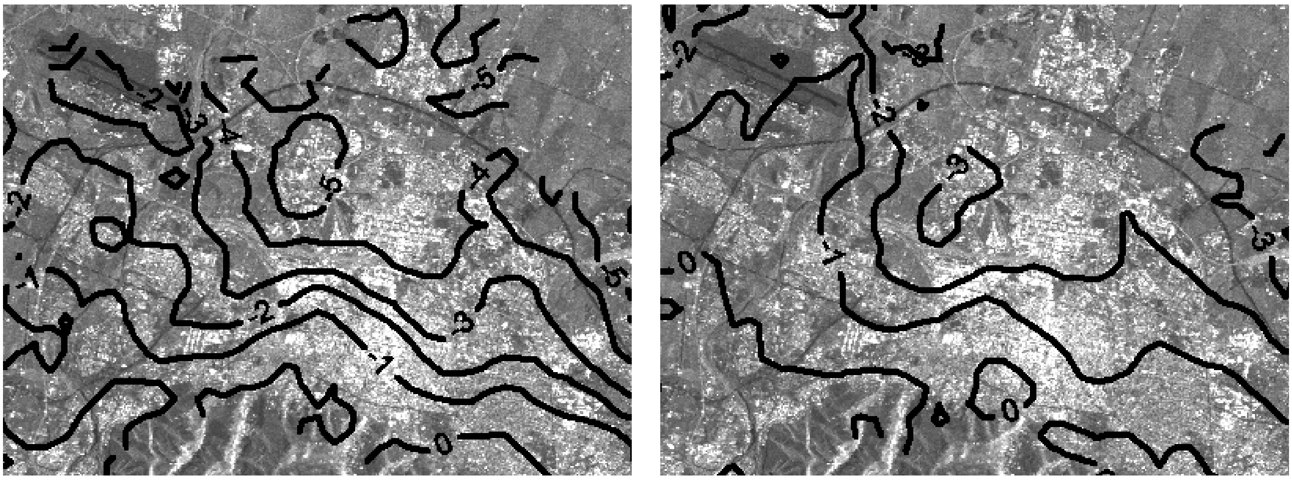

(a) (b)

Figure 4. SAR interferometric subsidence maps (in cm/year) in Bologna for the time periods 1992-1993 (a) and 1997-1998 (b). The backscattering coefficient is used as image brightness.

Euganean Geothermal Basin

Land subsidence of the Euganean Geothermal Basin, Italy, is related to the geothermal groundwater withdrawal. Precision levelling surveys conducted for the Commune di Abano Terme and the Regione del Veneto indicate maximum subsidence rates of 1 *cm/year* for the period up to 1991. After 1991 the subsidence velocity decreased as a consequence of a regulation of the groundwater withdrawal. In our investigation this case is used to analyze the feasibility of differential interferometric monitoring of slow subsidence velocities.

To map the expected low sub-*cm/year* subsidence velocity 10 interferograms in the time span 1992 to 1996 were selected. Interferogram stacking was used to generate a single subsidence map with a cumulative time interval of more than 20 years, allowing to reduce the expected velocity estimation error caused by atmospheric phase distortions to approximately 1 *mm/year*, a level which is significantly below the expected subsidence level of several *mm/year*.

The resulting interferometric deformation map shows a clear subsidence over Abano Terme with a maximum velocity of 4 *mm/year*, in agreement with the results of the last levelling surveys performed in 1991 and 1995 (Figure 4). The correspondence of the results of the two different surveying techniques is high, as confirmed by a direct quantitative validation of the interferometry based subsidence values along the levelling lines, an example of which is shown in Figure 5. For 17 points where we had values available from both surveying techniques the average difference of the vertical displacement velocity values was 0.2 mm/year with a standard deviation of 1.0 *mm/year*. The minimum and maximum differences were –1.5 *mm/year* and +2.2 *mm/year*, respectively. This result confirms the expected high accuracy achieved with the interferogram stacking technique. A more detailed description of this case was given by [5].

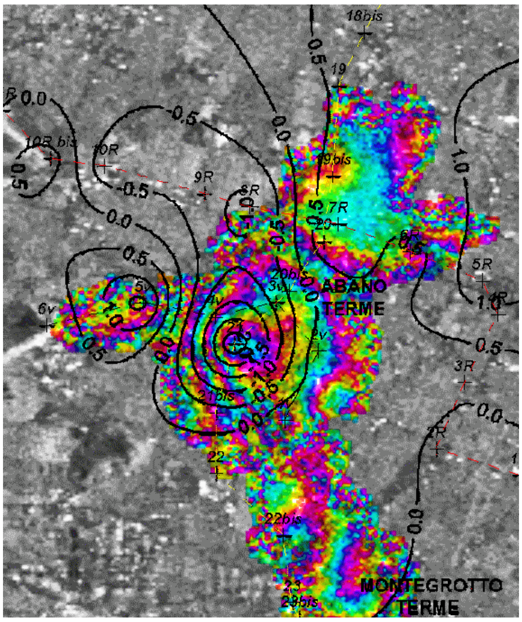

Figure 5. Vertical ground movements (in *mm/year)* from levelling surveys in 1991 and 1995 in the urban areas of Abano and Montegrotto Terme (data from Comune di Abano Terme and Regione del Veneto) superposed to the interferometric displacement velocity map for the interval 1992 to 1996. Also shown are the position of the levelling lines and benchmarks.

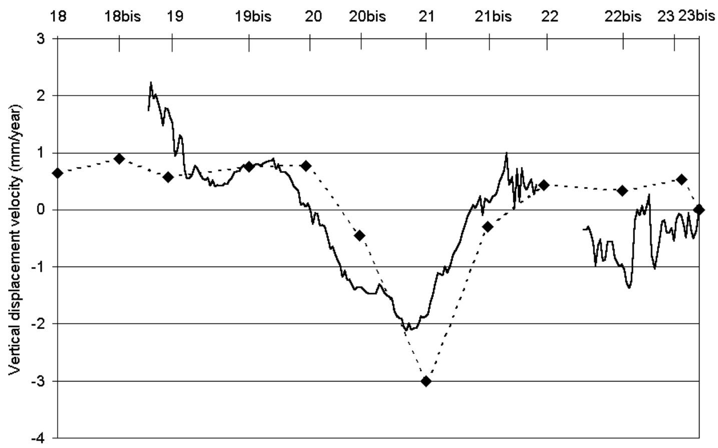

Figure 6. Profiles of the vertical displacement velocity from ERS SAR interferometry (continued line, period 1992-96) and levelling surveys (dotted line, period 1991-95, data from Comune di Abano Terme and Regione del Veneto) along the levelling line Abano Terme – Montegrotto Terme (yellow line in Figure 5).

SUBSIDENCE MONITORING WITH ENVISAT ASAR

The planned ENVISAT ASAR has the potential to maintain good data availability into the future. This will, nevertheless, strongly depend on the sensor operation strategy. Excellent orbit control, the operation of the ASAR in a single interferometric mode for most of the time and the acquisition of a large data archive are essential prerequisites for the subsidence application.

CONCLUSIONS

The feasibility of surface deformation mapping with ERS differential SAR interferometry was confirmed for a wide range of deformation velocities ranging from *m/year* (Ruhrgebiet, Mexico City) to *cm/year* (Bologna) and *mm/year* (Eugenean Geothermal Basin).

Data availability was found to be a limiting factor in the case of Mexico City. For the investigated European sites, on the other hand, a large number of ERS acquisition are available, allowing to optimize the data selection with respect to acquisition dates and interferometric baselines. For the planned future missions with SAR sensors which can be operated in a variety of modes (ENVISAT, ALOS) this means that the robustness and operationality of the subsidence application relies very much on the selection of a single interferometric mode for most of the time.

As demonstrated for the Euganean Geothermal Basin the interferogram stacking technique allows to reduce the errors caused by atmospheric distortions to a low level making the measurement of slow deformation velocities in the *mm/year* range feasible. The technique also allows to increase the temporal resolution of the monitoring, as demonstrated with the annual monitoring of the subsidence for Bologna.

The main limitations of the interferometric technique are the temporal decorrelation of the signal, which leads to an incomplete coverage with deformation information, with gaps mainly in forested and agricultural areas, and the well known problems of the SAR imaging geometry in areas of rugged topography, such as layover and radar shadow.

The interferometric technique was found to be fast, as demonstrated by the fact that we are still waiting for the levelling data to validate the latest Bologna results, and cost effective.

Considering the high quality of the results achieved for the investigated sites, the huge SAR data archive starting in 1991, the expected continued availability of new SAR data, and the maturity of the required data processing techniques, we conclude that differential SAR interferometry has a very high potential for operational mapping of land subsidence.

The complementarity of the interferometric technique with levelling surveys and GPS measurements suggests that the most effective monitoring strategy will be an integration of the different techniques.

ACKNOWLEDGMENTS

This work was supported by the ESA Data User Program (DUP). The Italian National Geologic Survey is acknowledged for the DEM.

REFERENCES

[1] Massonnet D., M. Rossi, C. Carmona, F. Adragna, G. Peltzer, K. Feigl, and T. Rabaute (1993), The displacement field of the Landers earthquake mapped by SAR interferometry, *Nature*, Vol. 364, No. 6433, pp. 138-142.

[2] Massonnet, D., P. Briole, and A. Arnaud (1995) Deflation of Mount Etna monitored by spaceborne radar interferometry, *Nature*, Vol 375, pp. 567-570.

[3] Goldstein R.M., R. Engelhardt, B. Kamb, and R. Frolich (1993), Satallite Radar Interferometry for Monitoring Ice Sheet Motion: Application to an Antarctic Ice Stream, *Science* Vol. 262, pp. 1525-1530, 3-dec-1993.

[4] Strozzi T. and U. Wegmüller (1999), Land Subsidence in Mexico City Mapped by ERS Differential SAR Interferometry, *Proc. IGARSS'99*, Hamburg, 28 June - 2 July.

[5] Strozzi T., L. Tosi, L. Carbognin, U. Wegmüller, and A. Galgaro (1999), Monitoring Land Subsidence in the Euganean Geothermal Basin with Differential SAR Interferometry, *Proc. Fringe'99*, Liège (B).

[6] Strozzi T., U. Wegmüller, and G. Bitelli (2000), Differential SAR interferometry for land subsidence mapping in Bologna, *Proc. SISOLS'2000*, Ravenna, Italy, 25-29 September.

[7] Wegmüller U., T. Strozzi, C. Werner, A. Wiesmann, N. Benecke, and V. Spreckels, “Monitoring of mining-induced surface deofrmation in the Ruhrgebiet (Germany) with SAR interferometry”, *Proc. IGARSS 2000*, Honolulu, USA, 24-28 July 2000.

[8] Strozzi T., U. Wegmüller, C. Werner, and A. Wiesmann, Measurement of slow uniform surface displacement with mm/year accuracy, *Proc. IGARSS'00*, Honolulu, USA, 24-28 July 2000.

[9] Wegmüller U., T. Strozzi, and L. Tosi, “Differential SAR interferometry for land subsidence monitoring: methodology and examples”, *Proc. SISOLS 2000*, Ravenna, Italy, 25 -29 September 2000.

[10] Wegmüller U. and T. Strozzi (1998), Characterization of differential interferometry approaches, EUSAR'98, 25-27 May, Friedrichshafen, Germany, *VDE-Verlag, ISBN 3-8007-2359-X*, pp. 237-240.

[11] Wegmüller U. and T. Strozzi, (1998), SAR interferometric and differential interferometric processing chain. *Proc. IGARSS'98*, Seattle, USA.